Finite size suppression of the weak field magnetoresistance of lightly phosphorous-doped silicon

Nicholas A. Porter[1, a)] and Christopher H. Marrows[1, b)]

School of Physics & Astronomy, University of Leeds, Leeds LS2 9JT, United Kingdom

(Dated: 6 March 2012)

We report magnetoresistance measurements of lightly phosphorous doped silicon in samples that are fabricated from silicon-on-insulator wafers and so confined in one dimension. All three principal magnetic field orientations were studied at 50 and 270 K for thicknesses between 1.5–530 μm, and as thin as 150 nm at 270 K. The weak field magnetoresistance was suppressed in the orientations with the field in the sample plane when the sample is thinner than ~ 1 μm at 270 K (~ 10 μm at 50 K). This suppression occurred for samples that are much thicker than the carrier mean free path and the Debye screening length, and the relevant lengthscale is instead the energy relaxation length.

PACS numbers: 72.80.Cw, 72.20.-i, 72.20.My.

[a)] n.a.porter@leeds.ac.uk

[b)] Author to whom correspondence should be addressed. c.h.marrows@leeds.ac.uk

I. INTRODUCTION

Silicon is by far the world's most commonplace semiconductor, and has been exploited both commercially and scientifically for decades in a wide range of applications. It was only recently, however, that a large magnetoresistance (MR) has been reported[1–4]. MR is the change in resistivity ρ of a material in a magnetic field B relative to the zero field resistivity: $\Delta\rho/\rho = [\rho(B) - \rho(0)]/\rho(0)$. The large transverse MR in silicon is linear in B at high field, and enhanced in high electric fields, yet seemingly intrinsic to the silicon itself. This phenomenon arises at low dopant densities[5,6], and is enhanced at low temperature T where the mobility μ is usually high.

In a purely free electron theory the MR is identically zero[7]. Meanwhile, semiclassical theory predicts the MR to be quadratic at weak magnetic fields and saturate in strong fields in systems with a closed Fermi surface[8], which still fails to describe the observed linear MR. This low-field quadratic MR is a result of the distribution of relaxation times so that the Lorentz force cannot be compensated by a single Hall field, and requires a component of magnetic field, $\mathbf{B}$, perpendicular to the current density, $\mathbf{J}$. Non-saturating linear MR is predicted in inhomogeneous semiconductors for which current paths can be convoluted[9,10] (or due to quantum effects in rare cases[11,12]). For any given field orientation, some component of the carrier's trajectory on its tortuous path will traverse magnetic field lines and be deflected by its influence. The resulting Hall voltages can appear at the longitudinal voltage contacts, giving rise to the linear MR at high fields. In this paper we observe both this high field linear MR and the low field quadratic MR, and focus our attention primarily on the latter.

Size effects in electron transport occur when samples become small enough that their size is comparable to characteristic lengthscales, for instance the carrier mean free path (MFP). In macroscopic and homogeneous materials, Matthiesen's rule tells us that the dominant influence on conductivity is from the scattering mechanism with the shortest relaxation time. When the sample dimensions are reduced the situation is more complex, since those mechanisms with the longest relaxation times have the longest diffusion lengths, and hence become comparable the sample size soonest. It is therefore these mechanisms that are the first to give rise to finite size effects as the sample dimensions are reduced. It is only when the dimensions become the order of tens of nanometers that the 'ordinary' size effects (those associated with the carrier MFP) usually become apparent[13,14]. Even relatively thick films

can have size effects on lengthscales associated with the longest relaxation times.

In solids there is a range of relaxation times, the differences between which can be extremely large, particularly in semiconductors, depending upon the electron property in question. The characteristic diffusion lengths vary according to $l \sim \sqrt{(D\tau)}$ where D is the diffusion coefficient and τ is the timescale in question. In general it is the momentum relaxation time that is the shortest of these timescales, $\tau_{\rm p} \sim 10^{-12}$ s. The associated diffusion length $l_{\rm p} \sim \sqrt{(D\tau_{\rm p})} \sim v\tau_{\rm p}$, where v is carrier velocity, is more commonly referred to as the MFP. Other relaxation times in solids are typically orders of magnitude larger. These include intervalley scattering, electron-hole recombination, dielectric, and energy relaxation.

Materials such as graphite[15] and bismuth[13,14] have exhibited reduced MR in confined geometries. These materials are renowned for their long MFP (of the order of microns), but in these materials care must also be taken to account for the large de Broglie wavelength that results from the extremely small effective masses of the carriers. It has been suggested that the large MR in phosphorous-doped silicon (Si:P) may be limited by the sample dimensions[3], but experiments directed at this specific point are still few in number. The silicon conduction energy surface has a significant effective mass (~ 0.4 of the free electron mass[7]) resulting in a much shorter de Broglie wavelength, ~ 10 nm at 50 K. The MFP can be estimated to be ~ 300 nm at 50 K[16]. Here we report the MR of Si:P studied in samples where the size was constrained in one dimension using silicon on insulator (SOI) wafers for all three principal orientations of **B**. We show that the MR for the two in-plane orientations is already suppressed at lengthscales as large as 10 μm at 50 K, far exceeding the MFP, and conclude that another lengthscale, that for carrier energy relaxation, plays the critical role in controlling the MR in this commonplace semiconductor.

II. EXPERIMENTAL DETAILS

The SOI wafers used in this study consisted of a thin *device* layer of Si:P of thickness t separated by a 0.3 – 0.5 μm silicon dioxide *buried oxide* (BOx) layer from a thick ($\sim 400\mu$m) Si:P *handle* as shown in Fig. 1(a). The Si:P handle had the same resistivity as the device. To verify the thicknesses of the wafers and to elucidate the effect of chemical etching, cross-sections were imaged using scanning electron microscopy (SEM). The etching was performed in 33 % (by weight) solution of potassium hydroxide (KOH), performed on a

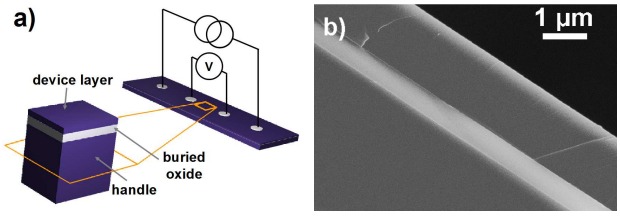

FIG. 1. (Color) SOI wafer sample structure. (a) Schematic of SOI wafer consisting of a thin *device* layer of doped silicon upon a *buried oxide* (BOx) typically 300–500 nm thick. This lay on a thick, doped silicon *handle*. Circular In contacts were made to the top and bottom surfaces of the stack. (b) SEM cross-section image of SOI wafer P after a 10 s etch in KOH, with the brighter layer being the SiO_2 BOx, and the handle at the bottom left of the image.

hotplate maintained at 80 °C. To make the cross-sections, approximately 2 mm high pillars of each SOI wafer were mechanically cleaved using a diamond scribe. The cleaved edge was then mounted on carbon tape such that the SOI wafer stood proud of the surface. The imaged cross-section was parallel to the holder, verified by excellent agreement of measured oxide thicknesses with the quoted values for all wafers. Fig. 1(b) shows an SEM image of wafer P (samples are defined in Table I) after a 10 s etch in KOH. For comparison with bulk Si:P we also measured a piece of ordinary (non-SOI) wafer, denoted sample K.

To ensure that the dopant density in the various commercial SOI device layers were consistent with one another, the room temperature resistivity, carrier density n, and mobility μ, of the wafers were obtained using standard van der Pauw techniques[17]. These measurements were performed on 3 mm × 3 mm square pieces of wafer, with Hall voltages recorded at $B = \pm 0.2$ T. Room temperature measurements of the SOI wafers are summarized in table I. Sample Q was prepared from the same wafer as sample P but was wet etched in KOH to reduce its thickness to 360 ± 20 nm. As can be seen from the Table, the mobilities of all the wafers were very similar, whilst the carriers densities varied by not much more than a factor of ~ 3. All the values of n are low enough that the samples are in the high intrinsic MR regime[6].

To study the MR in high fields the wafers were cleaved into (1.7 ± 0.2) mm × (7.5 ± 0.3) mm strips. Following a 4.5 nm depth Ar ion beam mill to ensure a clean, oxide free interface, 500 μm diameter In/Pt bilayer contacts were deposited *in situ* by DC magnetron sputtering through a shadow mask, each contact separated by 1.5 mm along the length. An

TABLE I. Electrical conduction properties of Si:P and SOI wafers measured by van der Pauw method at 298 ± 1 K.

device	t (μm)	ρ (Ωcm)	μ ($\mathrm{cm^2V^{-1}s^{-1}}$)	n ($\times 10^{15}$ $\mathrm{cm^{-3}}$)
K[a]	530 ± 50	3.6 ± 0.3	1390 ± 40	1.26 ± 0.08
L	100 ± 2	1.82 ± 0.04	1140 ± 50	3.2 ± 0.2
M	19.5 ± 0.5	3.20 ± 0.08	940 ± 50	2.2 ± 0.1
N	15.0 ± 0.5	2.00 ± 0.07	1090 ± 50	3.0 ± 0.1
O	2.0 ± 0.5	2.4 ± 0.6	890 ± 40	3.0 ± 0.8
P	1.5 ± 0.5	6 ± 2	1080 ± 50	1.1 ± 0.4
Q[b]	0.36 ± 0.02	6 ± 2	1080 ± 50	1.1 ± 0.4

[a] Bulk Si:P wafer.

[b] Sample Q was prepared from the same wafer as P (but thinned considerably following a KOH etch) and so ρ, n, and μ are taken to be the same in each case.

identically prepared contact was sputtered on the back of each sample to allow us to check that there was no significant current leakage to the handle wafer during measurement. The sample resistance was determined using standard four probe techniques maintaining ~ 5 mV between the voltage probes, small enough to remain in the ohmic regime at all magnetic fields (tested by measuring the current-voltage characteristic).

Sputtered contacts were ohmic at 270 K but became strongly rectifying at temperatures below ~ 200 K. To overcome this problem indium contacts were made by mechanically removing the native oxide and then alloying indium on the surface at 350 °C for 10 minutes in a high vacuum. These alternative contacts remained ohmic at low bias down to below 20 K as a result of the diffusion of In into the Si at the contacts. These samples were produced with a similar geometry to those with the sputtered contacts and were studied at 50 K.

III. MAGNETORESISTANCE MEASUREMENTS

Each strip of wafer was cooled to either 270 ± 1 K (sputtered contacts) or 50.0 ± 0.5 K (alloyed contacts) in a gas-flow cryostat and subjected to magnetic fields of up to 8 T.

The transverse, perpendicular, and longitudinal four-wire MR of the SOI wafers at both temperatures is displayed in Fig. 2 along with that of the bulk (non-SOI) wafer K. The weak-strong field crossover should occur at $B_{\rm SF} \sim 1/\mu$. This is the limit above which, on average, electrons complete more than one entire orbit of the Fermi surface prior to scattering. At 270 K, $B_{\rm SF} \sim 6.3$ T, and at 50 K, $B_{\rm SF} \sim 0.5$ T. Thus, at 270 K the lower mobility that results from enhanced acoustic phonon scattering provides MR that never fully passes into the strong field limit in our maximum available field of 8 T. The much lower value of $B_{\rm SF}$ at 50 K means that strong field MR occurs in that case.

In the transverse orientation [Fig. 2(a) & (d)] there was little difference in the MR of the various thickness samples as there is no confinement in the directions orthogonal to the applied field. These data are seemingly split into two slightly separate groupings at both 270 K and 50 K, but there is no clear trend with t as to which group any given sample should be in. The strong field MR was non-saturating and linear[4], reaching $\sim$ 600 % at 8 T and 50 K (these data are extended beyond the range plotted in Fig. 2(d)). In this transverse orientation, the magnetic field (**B**) and current density (**J**) vectors were mutually perpendicular but the aspect ratio normal the the magnetic field remained invariant between samples, leading to no obvious size effect.

This is not the case in the perpendicular orientation [Fig. 2(b) & (e)], where the carriers will experience strong confinement, since $\mathbf{J} \perp \mathbf{B}$, and a clear size effect is observed. At both measurement temperatures a reduction in the weak field MR was observed for thinner samples. At 50 K the characteristic linear strong field MR was also observed for $B \gtrsim B_{\rm SF} \approx$ 0.5 T. At 270 K the samples barely enter the strong field regime, but the MR can be see to starting to become linear at the highest measured fields.

In the longitudinal orientation [Fig. 2(c) & (e)], a dependence of MR on t is seen again. In this orientation there is no net component of **J** perpendicular to **B**, yet the tortuous motion of carriers in the inhomogeneous donor field provides a local component of the motion perpendicular to the magnetic field[4]. This MR is expected to saturate in high fields[18], which does appear to be taking place. Just as in the perpendicular orientation, the four wafers with $t \geq 15$ μm were approximately equivalent, whilst the wafers with thinner device layers (O, P, and Q) showed a clear size effect, with a reduction in MR at 8 T with decreasing t. All the samples have roughly the same high-field Kohler slope, and so this reduction mostly occurred in the weak field regime.

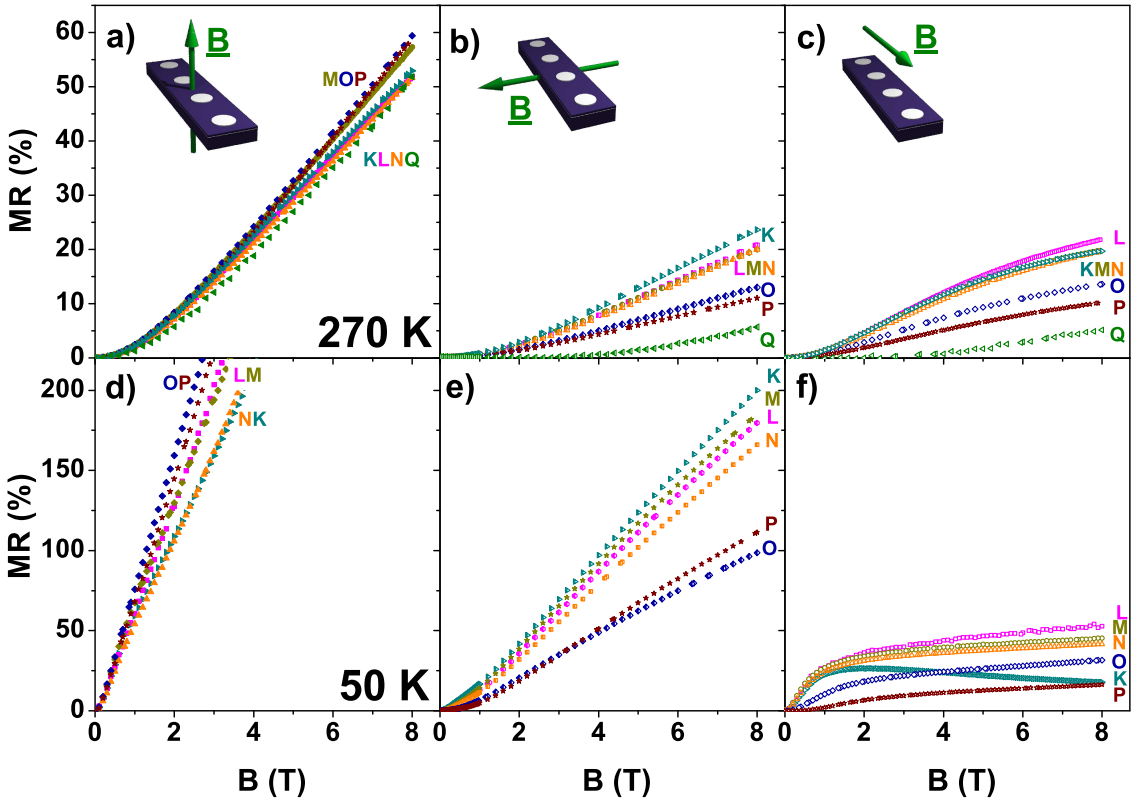

FIG. 2. (Color) Four-wire MR of samples with sputtered contacts at 270 K (a)–(c) and with alloyed contacts at 50 K (d)–(f). The measurement geometries are depicted in the inset diagrams which represent: transverse (a) & (d), perpendicular (b) & (e) and longitudinal (c) & (f). In each case, the current flows along the length of the strip between the outermost contacts. The thicknesses t of samples K (▶), L (■), M (●), N (▲), O (♦), P (★), and Q (◀) are given in Table I. When magnetic field and current are orthogonal, a linear positive MR was measured in strong fields. In longitudinal fields the MR could be considered as tending towards saturation. At both temperatures the transverse MR presents no obvious trend with thickness of the device. In contrast both perpendicular and longitudinal fields were strongly thickness dependent suggesting that the MR is gradually suppressed as the Si:P device layer becomes thinner.

We now turn to the data for the longitudinal MR measured at the colder temperature of 50 K, using the samples with the alloyed contacts, where a qualitatively similar picture emerges. (Sample Q, the thinnest, could not be measured in this experiment as it became too resistive when cooled.) In the weak field limit for $B \lesssim 0.5$ T the MR was relatively weakly affected by thickness for $t \gtrsim 15$ μm. At higher fields the MR is progressively suppressed

for smaller thicknesses, with very significant reductions in samples O and P. Once again, in strong fields the Kohler slope from the four wire measurement was similar for all the SOI samples, and small, indicating that saturation is taking place. Slight discrepancies may be associated with differences in the width of samples[4,19]. Sample K, the bulk wafer, does not follow this pattern, and in particular a negative high field Kohler slope was observed, the cause of which is not clear. It is possible that in the thicker samples an uneven current distribution occurs perpendicular to the plane of the current leads, which can result in a reduced effective resistance at high magnetic fields[20]. The electrode separation in these samples was $\sim$ 1.5 mm, only three times the thickness of sample K for which the most significant strong field MR distortion was measured. For samples thinner than 100 μm the current would have redistributed more effectively from the sample surface. This hypothesis could be tested by altering the electrode separation to see the influence on the negative strong field MR gradient.

The MFP, $l_{\rm p}$, of electrons accelerated in weak electric fields can be determined from the electron velocity once the mobility is known. In degenerate semiconductors this velocity is the Fermi velocity, $\sqrt{2\varepsilon_{\rm F}/m^\star}$, where $\varepsilon_{\rm F}$ is the Fermi energy and $m^\star$ the effective mass of the electron, but in the lightly doped silicon used here the thermal velocity, $\sqrt{3k_{\rm B}T/m^\star}$, is appropriate[16]. (Here, $k_{\rm B}$ is the Boltzmann constant.) Hence, the mean free path is given by

$$l_{\rm p} = \frac{\mu}{e}\left(3m^\star k_{\rm B}T\right)^{\frac{1}{2}}, \tag{1}$$

where e is the charge of the electron. By using the mobility determined from the van der Pauw measurements, an appropriate effective mass ($m^\star \sim 0.4$ free electron masses in Si:P[7]), the bulk MFP at 270 K was found to be $l_{\rm p} \approx 64$ nm. For all samples in table I the device thickness far exceeded this MFP illustrating that the finite-size suppression of the longitudinal and perpendicular MR observed in Fig. 2 is caused by some alternative scattering mechanism.

We therefore made a further sample from the same SOI wafer used to prepare samples P and Q in order to study the MR in an even thinner limit. An SEM image of an SOI wafer after a 35 s KOH etch is shown in Fig. 3(a). The thickness of the device after etching was $t = 147 \pm 5$ nm. Surface contacts were sputtered in the same way as for the previous samples. Only two-wire DC measurements of this sample were possible due to its very high resistance, and the MR at 270 K is shown in Fig. 3(b). (Such a thin sample was too resistive

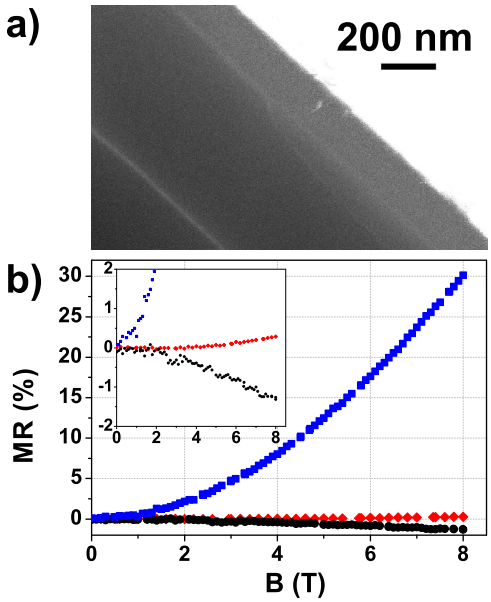

FIG. 3. (Color) (a) SEM cross-section image shows a $\sim$ 150 nm device after KOH etch. (b) Two-wire MR in SOI wafer P after an etch in KOH for 35 s in transverse (■), perpendicular (♦) and longitudinal (•) field orientations measured at 270 K. The inset shows a magnification of the low MR data.

to be measurable at all at 50 K.) For this sample $t/l_{\rm p} \sim 2.6$ at 270 K and the device layer can still be considered to be three-dimensional[21].

The positive transverse MR measured by the two probe method was quadratic in B over the entire field range and about a factor of two smaller in magnitude than the thicker samples. We attribute this reduction to the surface scattering that arises when t is of the order of the MFP[22,23], which increases the overall resistivity.

The perpendicular MR is also positive and quadratic in B, but is very small, < 1 % in 8 T, as can be seen in the inset to Fig. 3(b). This is the extreme limit of the finite-size effect observed in the perpendicular data in Fig. 2(b) & (e), the thinness of the sample has almost completely suppressed the MR — it is almost two orders of magnitude smaller than in the bulk wafer K.

In the longitudinal field the MR was very small and negative, with a 1.3 % reduction in the device resistance in an 8 T field. The inset of Fig. 3(b) shows the negative MR data magnified to emphasize the change. In thin films, when the electric and magnetic fields are parallel and $t \lesssim l_{\rm p}$, the Lorentz force curls up the electron trajectories and so extends the

effective mean free path by reducing surface scattering. Meanwhile, the the component of their velocity along the electric field direction is unaffected. Negative MR reported in thin films and wires in longitudinal fields is generally explained by this mechanism[18,24,25].

This weak negative contribution to the MR is unlikely to influence devices for $t \gg l_{\rm p}$ and the size effects associated with momentum relaxation can be assumed to be absent in the four-wire MR data shown in Fig. 2. Other scattering mechanisms are likely to be the important influence on carrier transport on these lengthscales. We now turn our attention to what these might be.

IV. DISCUSSION

The reduction of weak field MR in our samples was quantified by fitting the quadratic dependence of the MR for weak B using the relationship $\Delta\rho/\rho = (aB)^2$. The coefficients obtained, a, which have dimensions of mobility, are plotted as a function of Si:P thickness t in Fig. 4 for all the data described above. The reduction in MR (smaller values of a) can be seen to take place in the perpendicular and longitudinal geometries for samples where the thickness is ~ 1 μm at 270 K and ~ 10 μm at 50 K. (There is only a very weak dependence of the MR on t in the transverse case.) These lengthscales are an order of magnitude greater than $l_{\rm p}$, with the calculated values marked as vertical dotted lines. This implies that a lengthscale other than the MFP must be responsible for the size effect in these cases[26,27].

One possibility is the Debye screening length, $\lambda_{\rm d}$. Ciccarelli *et al.* measured the MR of narrow Si devices in high electric fields[3]. They observed an order of magnitude reduction in transverse MR at 4.2 K when their devices were reduced from 50×280 μm^2 to 5×5 μm^2. They suggested that this was because the sample dimensions were comparable to this screening length, which then controls when the Mott-Gurney space charge accumulation will be established, which boosts the magnetoresistance[2]. This is not relevant to our results, which are all measured in the ohmic regime. The Debye screening length depends upon the density of free carriers and the Si:P permittivity, ϵ, and is defined as[29] $\lambda_{\rm d} = \sqrt{\epsilon k_{\rm B} T/(ne^2)}$. We also mark this lengthscale on Fig. 4, and can see that the reduction in transverse and longitudinal MR sets in whilst t is still an order of magnitude greater than $\lambda_{\rm d}$, leading us to also reject this as the relevant lengthscale.

Another candidate lengthscale for the MR reduction was proposed by Gribnikov and

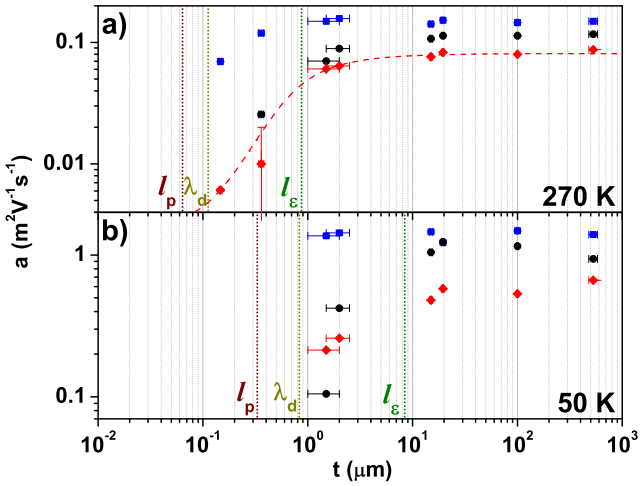

FIG. 4. (Color) Variation in the weak field MR coefficient, a, as a function of thickness at (a) 270 K and (b) 50 K measured in three field orientations: transverse (■), perpendicular (♦) and longitudinal (•). The vertical dotted lines represent the MFP, $l_{\rm p}$, screening length, $\lambda_{\rm d}$, and energy relaxation length, l_ε, at each temperature. There was little influence on the transverse field upon thickness. In perpendicular and longitudinal fields the value of a tends to the bulk value when $t > l_\varepsilon$. The dashed line is a fit of the leading term in the model of Gribnikov and Mel'nikov[28] to the perpendicular data.

Mel'nikov[28], and was subsequently used by Klimovskaya *et al.*[30] to explain their experimental results on n-Si films. It is the energy relaxation length, l_ε. The physical mechanism at play is that electrons with different energies will experience different Lorentz forces in the same field due their different velocities and hence become spatially separated. The electrons can re-equilibrate in bulk material but are unable to do so within l_ε of the surface, giving rise to electron temperature gradients that result in a thermoelectric emf. This drives in internal current that is itself deflected by the magnetic field through the Nernst effect, and the resulting voltage will be detected at the sample voltage probes, partially canceling the MR.

Klimovskaya *et al.* suggested that the increased anisotropy in MR at 30 K for inhomogeneous n-type silicon for relatively 'thick' 40 μm samples arose because the sample dimensions shrank to become comparable to the energy relaxation length. The associated timescale, the energy relaxation time, τ_ε, is the timescale of re-establishing the average charge carrier energy[19], i.e. the time taken for excited carriers to reach thermal equilibrium with the lattice. To transfer energy to the lattice, inelastic scattering processes are required. The

majority of scattering is elastic so many scattering events (with a mean transit time $\bar{\tau}$) usually occur before a hot electron relaxes, so that $\tau_\varepsilon > \bar{\tau}$. For 'warm' electrons, designated so because they have been accelerated by weak electric fields, the energy relaxation time has been measured[31,32]. Extrapolating from the data in Ref. 32, gathered between 77 K and 180 K, we estimate the energy relaxation times for n-type silicon at 50 and 270 K to be 137 and 6.1 ps respectively. The energy relaxation lengths for electrons, l_ε, are hence estimated to be 8.4 μm at 50 K and 0.87 μm at 270 K. These lengthscales are also shown in Fig. 4 for the two temperatures. We can see that the weak field MR coefficient a drops when $t \lesssim l_\varepsilon$ for the two geometries in which the field lies in the sample plane and there is a size effect, but is close to constant once t exceeds this length.

Gribnikov and Mel'nikov only treated the perpendicular case in detail in their theory[28]. They predict that the magnetoconductance $\Delta\sigma/\sigma \approx -\Delta\rho/\rho$ has a finite-size correction for which the leading term has the form $\tanh\delta/\delta$ (where $\delta = t/l_\varepsilon$) in the limit of equal and opposite modifications of the electron temperature profile at the top and bottom film surfaces (reasonable here as inequivalence will lead to rectification behavior which we do not observe in our experiments). The dashed line in Fig. 4(a) is a fit to our perpendicular 270 K data (both two and four-wire) using this finite-size correction, which returns $l_\varepsilon = 0.8 \pm 0.1$ μm, in good agreement with our estimate of 0.87 μm given above. (Fitting the 50 K data is problematic since we lack data points for low t.)

The effect should not arise in the transverse geometry since the sample size greatly exceeds l_ε in both directions orthogonal to the field, and we indeed see no significant t dependence for the data taken in this geometry in Fig. 4. However, the it should also be ruled out in a purely longitudinal geometry, as there are no Lorentz forces when $\mathbf{J}||\mathbf{B}$, nevertheless a clear finite size effect in the weak field MR is observed in our data. The linear MR observed in high fields (both here and in Si:P samples with similar doping levels[4]) indicates that there are statistical fluctuations in the donor density that will affect the local current flow direction[9]. We can therefore expect that there will be many regions where the measurement geometry envisaged by Gribnikov and Mel'nikov can locally be realized. We suggest that if many such regions can be found within a distance of l_ε then lateral self-averaging will occur in such as way as to allow the size effect to be observed, as we do.

V. CONCLUSION

In conclusion, we have demonstrated that whilst the transverse MR is almost entirely unaffected, the longitudinal and perpendicular quadratic MR for weak fields is suppressed as the thickness of the Si:P device layer is reduced below about 1 μm at 270 K (about 10 μm at 50K). The MFP and Debye screening length are much shorter than these lengthscales, but they are close to the energy relaxation lengths at these temperatures, indicating that this scale plays the critical role in MR suppression, which we attribute to local electron temperature gradients within l_ε of the surface. Increasing the relaxation rate for electron energy through additional inelastic scattering would allow weak-field MR to be observed in nanoscale devices based on Si, which is currently prevented by these size effects.

ACKNOWLEDGMENTS

The authors would like to acknowledge research funding from the (UK) EPSRC.

REFERENCES

[1]J. J. H. M. Schoonus, F. L. Bloom, W. Wagemans, H. J. M. Swagten, and B. Koopmans, Phys. Rev. Lett. **100**, 127202 (2008).

[2]M. P. Delmo, S. Yamamoto, S. Kasai, T. Ono, and K. Kobayashi, Nature (London) **457**, 1112 (2009).

[3]C. Ciccarelli, B. G. Park, S. Ogawa, A. J. Ferguson, and J. Wunderlich, Appl. Phys. Lett. **97**, 082106 (2010).

[4]N. A. Porter and C. H. Marrows, "Linear magnetoresistance in commercial n-type silicon due to inhomogeneous doping," (2011), arXiv:1105.2174 [cond-mat.mtrl-sci].

[5]J. J. H. M. Schoonus, P. P. J. Haazen, H. J. M. Swagten, and B. Koopmans, J. Phys. D: Appl. Phys. **42**, 185011 (2009).

[6]N. A. Porter and C. H. Marrows, J. Appl. Phys. **109**, 07C703 (2011).

[7]N. W. Ashcroft and N. D. Mermin, *Solid State Physics* (Harcourt College Publishers, Fort Worth, 1976).

[8]A. Sommerfeld and N. H. Frank, Rev. Mod. Phys. **3**, 1 (1931).

[9]C. Herring, J. Appl. Phys. **31**, 1939 (1960).

[10]M. M. Parish and P. B. Littlewood, Nature (London) **426**, 162 (2003).

[11]A. A. Abrikosov, J. Phys. A: Math. Gen. **36**, 9119 (2003).

[12]A. L. Friedman, J. L. Tedesco, P. M. Campbell, J. C. Culbertson, E. Aifer, K. Perkins, R. L. Myers-Ward, J. K. Hite, C. R. E. Jr., G. G. Jernigan, and D. K. Gaskill, Nano. Lett. **10**, 3962 (2010).

[13]F. Y. Yang, K. Liu, K. Hong, D. H. Reich, P. C. Searson, and C. L. Chien, Science **284**, 1335 (1999).

[14]F. Y. Yang, G. J. Strijkers, K. Hong, D. H. Reich, P. C. Searson, and C. L. Chien, J. Appl. Phys. **89**, 7206 (2001).

[15]J. C. González, M. Muñoz, N. García, J. Barzola-Quiquia, D. Spoddig, K. Schindler, and P. Esquinazi, Phys. Rev. Lett. **99**, 216601 (2007).

[16]L. Weber and E. Gmelin, Appl. Phys. A **53**, 136 (1991).

[17]L. J. van der Pauw, Philips Tech. Rev. **20**, 220 (1958).

[18]A. B. Pippard, *Magnetoresistance in Metals* (Cambridge University Press, Cambridge, 1989).

[19]R. S. Popovic, *Hall Effect Devices*, 2nd ed. (Institute of Physics Publishing, London, 2004).

[20]J. Hu, T. F. Rosenbaum, and J. B. Betts, Phys. Rev. Lett. **95**, 186603 (2005).

[21]A. S. Troup, J. Wunderlich, and D. A. Williams, Journal of Applied Physics **101**, 033701 (2007).

[22]K. Fuchs, Proc. Cambridge Phil. Soc. **34**, 100 (1938).

[23]E. H. Sondheimer, Phys. Rev. **80**, 401 (1950).

[24]R. G. Chambers, Proc. Roy. Soc. Lond. A Mat. **202**, 378 (1950).

[25]Y.-H. Kao, Phys. Rev. **138**, A1412 (1965).

[26]V. V. Mitin and N. A. Prima, Phys. Status Solidi B **58**, 809 (1973).

[27]B. P. Zot'ev, a. V. Skubnevskii, and A. T. Dudarev, Russ. Phys. J. **18**, 691 (1975).

[28]A. S. Gribnikov and V. I. Mel'nikov, Sov. Phys. JETP **24**, 1282 (1967).

[29]S. M. Sze, *Physics of Semiconductor Devices*, 2nd ed. (John Wiley and Sons, Hoboken, New Jersey, 1981) p. 31.

[30]A. I. Klimovskaya, O. V. Snitko, and S. I. Kirillova, ZhETF **11**, 119 (1970).

[31]C. Jacoboni, C. Canali, G. Ottaviani, and A. A. Quaranta, Solid-State Electron. **20**, 77 (1977).

[32]K. Hess and K. Seeger, Z. Phys. A Hadron. Nucl. **218**, 431 (1969).